Three-Dimensional Network of Inductively Coupled Josephson Junctions as a Vectorial Magnetic Field Sensor

T. Di Matteo, J. Paasi, A. Tuohimaa
Laboratory of Electricity and Magnetism, Tampere University of Technology, FIN-33101 Tampere, Finland

R. De Luca
INFM-Dipartimento di Fisica, Universitá degli Studi di Salerno, I-84081 Baronissi (Salerno), Italy.

Abstract—**We study the response of a current biased three-dimensional cubic network of inductively coupled Josephson junctions for different directions of the applied magnetic field by means of numerical simulations. We discuss the feasibility of these systems to be used as sensitive vectorial magnetic field sensors.**

I. Introduction

There is widespread general interest in sensitive magnetic field sensors. Nowadays, these devices are used in a great variety of applications, from biomagnetic measurements to maintenance testing of aircraft [1]-[5]. A good example of widely used sensitive sensors is given by SQUIDS [6],[7]. Their planar geometry, however, allows measurement of one magnetic field component only, while the physical quantity to be detected is a vector. As a candidate for a sensitive vectorial magnetic field sensor we have considered the three-dimensional cubic network of inductively coupled Josephson junctions (JJs) shown in Fig. 1. In our system, consisting of a cube containing twelve junctions, the bias current I_{bias} is injected from the node at position $\vec{r}_1$=(a,0,a), where a is the side of a single square loop, and is drawn from the node at the position $\vec{r}_2$=(0,a,0). The external magnetic field $\vec{H}$ is directed in space as shown in the upper right inset of Fig. 1. Each branch of the system carries a current $i_\xi(\vec{r})$, where ξ denotes the axis to which the branch is parallel and $\vec{r}$ is the position in space of the starting point of the branch itself, taken to be oriented according to the positive ξ-direction. A voltage $V_\xi(\vec{r})$ can be detected across each branch.

We study the magnetic field response of the system by numerically evaluating the time average of the voltages $V_\xi(\vec{r})$ as functions of the magnetic field amplitude for fixed values of I_{bias} and of the magnetic field direction. By analogy with the well-known operation of a dc SQUID, we argue that the system could be adopted as a sensitive vectorial magnetic field sensor.

Manuscript received September 14, 1998.

II. The Equations

A set of coupled non-linear differential equations, describing the dynamics of the gauge-invariant phase differences $\varphi_\xi(\vec{r})$ across the junctions in the cubic network, can be obtained by means of the RSJ model [8]. By introducing the non-linear Josephson operator O_J, such that:

$$O_J(\cdot) = \frac{\Phi_0}{2\pi R}\frac{d}{dt}(\cdot) + I_{J0}sin(\cdot), \tag{1}$$

where Φ_0 is the elementary flux quantum and I_{J0} and R are the maximum Josephson current and the resistive parameter of the junction, respectively, we can write:

$$O_J[\varphi_\xi(\vec{r})] = i_\xi(\vec{r}). \tag{2}$$

In (1) we have implicitly assumed the system to be homogeneous. The currents $i_\xi(\vec{r})$ can be expressed in terms of the fluxes $\Phi_{\mu\nu}$ linked to the six loops. Here, the indices $(\mu\nu)$=(yz), (zx), (xy) denote the fluxes linked to the loops lying in the homologous planes, so that:

$$\Phi_{\mu\nu}(\vec{r}) = lI_{\mu\nu}(\vec{r}) + MI_{\mu\nu}(\vec{r}+a\hat{\xi}) + \mu_0\vec{H}\cdot\vec{S}_{\mu\nu}(\vec{r}) \tag{3}$$

$$\Phi_{\mu\nu}(\vec{r}+a\hat{\xi}) = lI_{\mu\nu}(\vec{r}+a\hat{\xi}) + MI_{\mu\nu}(\vec{r}) + \mu_0\vec{H}\cdot\vec{S}_{\mu\nu}(\vec{r}+a\hat{\xi}) \tag{4}$$

where

$$I_{\mu\nu}(\vec{r}) = i_\nu(\vec{r}+a\hat{\mu}) - i_\nu(\vec{r}) - i_\mu(\vec{r}+a\hat{\nu}) + i_\mu(\vec{r}) \tag{5}$$

and $I_{\mu\nu}(\vec{r}+a\hat{\xi})$ is obtained from (5) by letting $(\vec{r})\rightarrow(\vec{r}+a\hat{\xi})$. In (3), (4) $\vec{S}_{\mu\nu}$ is the area vector pertaining to the $(\mu\nu)$-loop, l is the self-inductance coefficient of each branch in the $(\mu\nu)$-loop and M is the mutual inductance coefficient between this loop and a non-orthogonal branch.

Finally, the fluxes can be related to the phase differences $\varphi_\xi(\vec{r})$ by means of the fluxoid quantization relations [9]:

$$2\pi\frac{\Phi_{\mu\nu}(\vec{r})}{\Phi_0} = 2\pi n_{\mu\nu}(\vec{r}) + \Theta_{\mu\nu} \tag{6}$$

1051-8223/99$10.00

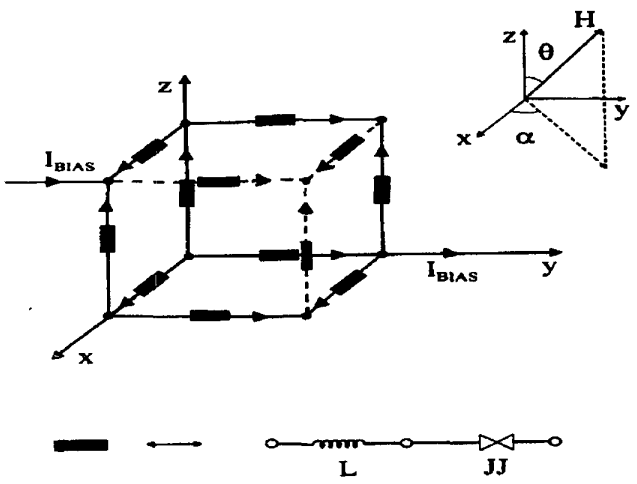

Fig. 1. Three-dimensional cubic network of inductively coupled Josephson junctions. Each branch contains a Josephson junction and an inductor as shown in the bottom inset. The field direction is indicated in the upper right inset and the current bias is injected from the (a, 0, a)-node and is drawn from the (0, a, 0)-node.

where $n_{\mu\nu}$'s are integers and

$$\Theta_{\mu\nu} = \varphi_\mu(\vec{r} + a\hat{\nu}) - \varphi_\mu(\vec{r}) - \varphi_\nu(\vec{r} + a\hat{\mu}) + \varphi_\nu(\vec{r}). \quad (7)$$

However, given that in the cubic circuital system we have eight nodes, we might express all the $i_\xi(\vec{r})$ in terms of a chosen set of five independent currents. In this paper we have chosen the following: $i_x(\vec{r})$, $i_x(\vec{r} + a\hat{y})$, $i_x(\vec{r} + a\hat{y} + a\hat{z})$, $i_y(\vec{r} + a\hat{z})$, $i_z(\vec{r} + a\hat{x})$. In this way, (3), (4) can be inverted to give the independent currents in terms of the forcing terms I_{bias} and $\mu_0\vec{H} \cdot \vec{S}_{\mu\nu}$ and of the fluxes, which can be expressed in terms of the phase variables $\varphi_\xi(\vec{r})$ by (6),(7). Therefore, (2) represent the non-linear ordinary differential equations describing the dynamics of the phase variables and, thus, of the observable physical quantities, for different values of the forcing terms. In particular, then, the voltages $V_\xi(\vec{r})$ can be expressed as follows [8]:

$$V_\xi(\vec{r}) = l\frac{di_\xi(\vec{r})}{dt} + \frac{\Phi_0}{2\pi}\frac{d\varphi_\xi(\vec{r})}{dt}. \quad (8)$$

III. The Results

Integration of the non-linear ordinary differential equations (2) gives us complete knowledge of the time evolution of the macroscopic physical quantities as, for example, the normalized voltages $v_\xi(\vec{r})$=$V_\xi(\vec{r})/RI_{J0}$. In order to relate our numerical analysis to experimentally detectable quantities, we need to average the voltages over the time variable t, in such a way that

$$< v_\xi(\vec{r}) >= \frac{1}{T}\int_{t_0}^{t_0+T} v_\xi(\vec{r})dt, \quad (9)$$

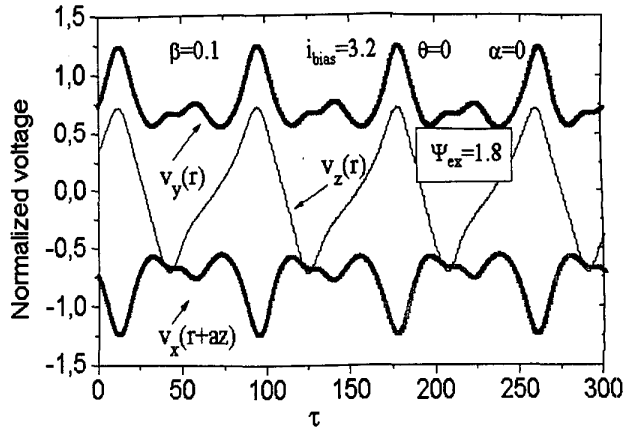

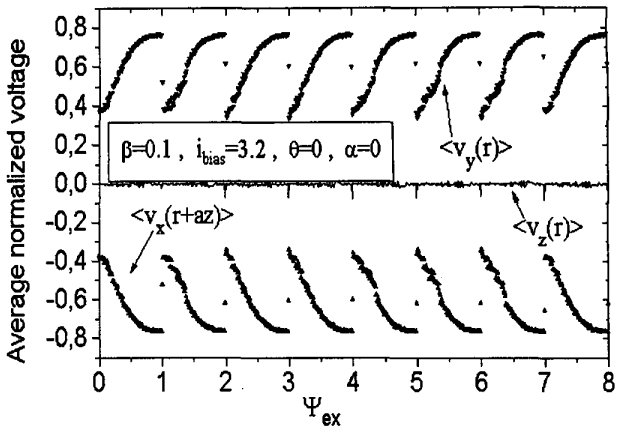

Fig. 2. a)Time dependence of the normalized voltages $v_x(\vec{r} + a\hat{z})$, $v_y(\vec{r})$, $v_z(\vec{r})$ for $\alpha = 0$, $\theta = 0$, $\beta = 0.1$, $i_{bias} = 3.2$ and $\Psi_{ex} = 1.8$. The normalized time τ is $(2\pi Rt)/l$.
b)Average normalized voltage $< v_x(\vec{r} + a\hat{z}) >$, $< v_y(\vec{r}) >$ and $< v_z(\vec{r}) >$ versus the normalized applied flux Ψ_{ex} for α=0, θ=0, β = 0.1 and $i_{bias} = 3.2$.

where $< v_\xi(\vec{r}) >$ is the observable quantity related to $v_\xi(\vec{r})$. Numerically, the averaging can be done either by knowledge of the period of $v_\xi(\vec{r})$, if it exists, or by integrating the function $v_\xi(\vec{r})$ over a long enough period of time T.

The set of equations given by (2)-(8) has been integrated by a standard fourth order Runge-Kutta algorithm. Care has been taken to let the forcing term vary by small enough increments, letting the system reach its stationary state corresponding to the augmented value of the external current bias or applied field, before a new increment of the same quantity was performed. The first $< v_\xi >$ vs. Ψ_{ex}=$\frac{\mu_0 H S_0}{\Phi_0}$ curves, S_0 being the area of a single square loop, are given in Figs. 2-3 for a given value of the parameter $\beta = \frac{lI_{J0}}{\Phi_0}$, for $i_{bias} = \frac{I_{bias}}{I_{J0}} = 3.2$ and for two different field directions (α=0; θ=0, $\pi/4$). In particular, in Figs. 2a, 3a we show the time dependence of the normalized voltages $v_x(\vec{r} + a\hat{z})$, $v_y(\vec{r})$ and $v_z(\vec{r})$, for

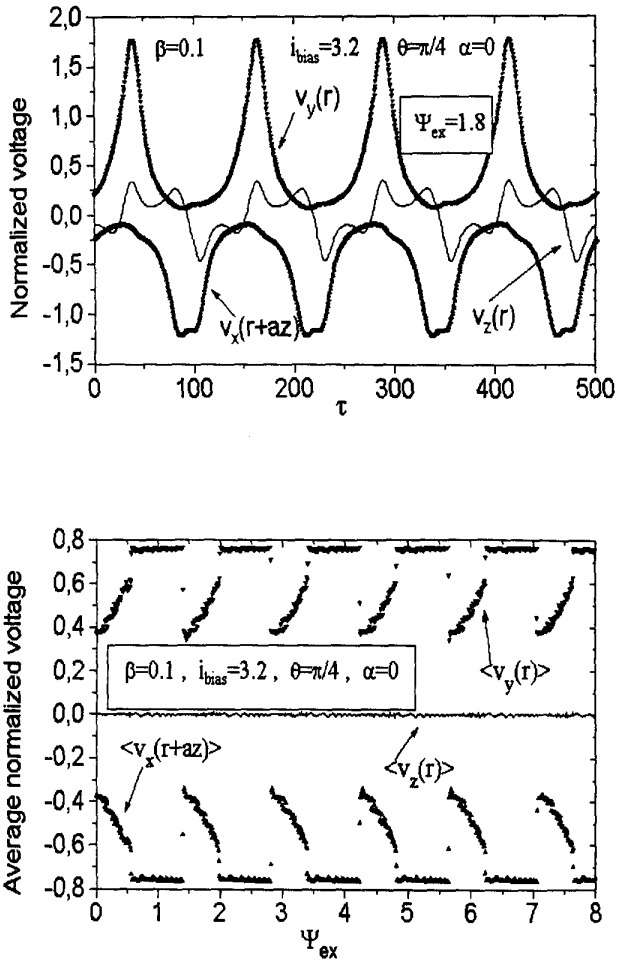

Fig. 3. a)Time dependence of the normalized voltages $v_x(\vec{r}+a\hat{z})$, $v_y(\vec{r})$, $v_z(\vec{r})$ for $\alpha=0$, $\theta=\pi/4$, $\beta=0.1$, $i_{bias}=3.2$ and $\Psi_{ex}=1.8$. The normalized time τ is $(2\pi Rt)/l$.
b)Average normalized voltage $< v_x(\vec{r}+a\hat{z}) >$, $< v_y(\vec{r}) >$ and $< v_z(\vec{r}) >$ versus the normalized applied flux Ψ_{ex} for α=0, θ=$\pi/4$, $\beta=0.1$ and $i_{bias}=3.2$.

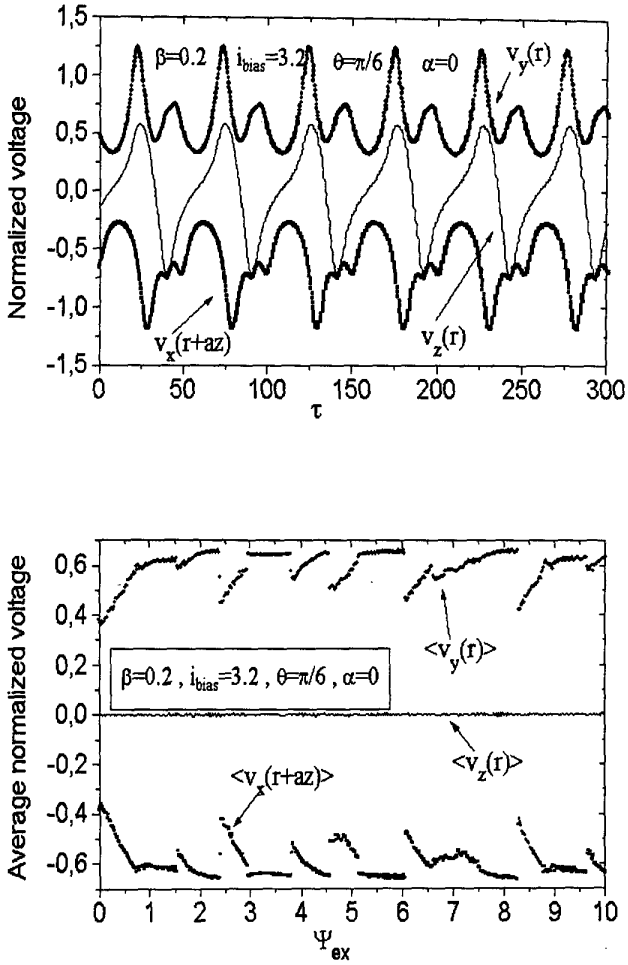

Fig. 4. a)Time dependence of the normalized voltages $v_x(\vec{r}+a\hat{z})$, $v_y(\vec{r})$, $v_z(\vec{r})$ for $\alpha=0$, $\theta=\pi/6$, $\beta=0.2$, $i_{bias}=3.2$ and $\Psi_{ex}=1.8$. The normalized time τ is $(2\pi Rt)/l$.
b)Average normalized voltage $< v_x(\vec{r}+a\hat{z}) >$, $< v_y(\vec{r}) >$ and $< v_z(\vec{r}) >$ versus the normalized applied flux Ψ_{ex} for α=0, θ=$\pi/6$, $\beta=0.2$ and $i_{bias}=3.2$.

$i_{bias}=3.2$, $\Psi_{ex}=1.8$, $\alpha=0$ and, respectively, for the angles $\theta=0$ and $\pi/4$.

We note that Figs. 2*a* and 3*a* show a very clear time periodicity. In Figs. 2*b* and 3*b*, on the other hand, we report the time-averaged quantities of the normalized voltages $< v_x(\vec{r}+a\hat{z}) >$, $< v_y(\vec{r}) >$ and $< v_z(\vec{r}) >$ vs. Ψ_{ex} for the same value of i_{bias} and for the same field directions as in Figs. 2*a*, 3*a*.

These curves are particularly interesting, since they show that the system follows regular $< v_\xi(\vec{r}) >$ vs. Ψ_{ex} patterns for external fields along these two directions. The periodicity $\Delta\Psi_{ex}$ with which these patterns appear can be related to the invariance of the stationary states of the system with respect to the external forcing term Ψ_{ex} [6]. Let us transform the phases, the fluxes and the $n_{\mu\nu}$ integers as follows:

$$\varphi_\mu(\vec{r}),\varphi_\mu(\vec{r}+a\hat{\nu})\rightarrow\varphi_\mu(\vec{r})+2\pi,\varphi_\mu(\vec{r}+a\hat{\nu})+2\pi$$

$$\varphi_\nu(\vec{r}),\varphi_\nu(\vec{r}+a\hat{\mu})\rightarrow\varphi_\nu(\vec{r})+2\pi,\varphi_\nu(\vec{r}+a\hat{\mu})+2\pi \quad (10)$$
$$\Phi_{\mu\nu}(\vec{r})\rightarrow\Phi_{\mu\nu}(\vec{r})+k_\xi\Phi_0\ ;\ n_{\mu\nu}(\vec{r})\rightarrow n_{\mu\nu}(\vec{r})+k_\xi$$

where the k_ξ' s are integers and $\xi\neq\mu,\nu$. Let also the corresponding translated quantities along $\xi\neq\mu,\nu$ be transformed in a similar way. Now, in order to keep the stationary equations for the system invariant, we need to let

$$\frac{\mu_0\vec{H}\vec{S}_{\mu\nu}}{\Phi_0}\rightarrow\frac{\mu_0\vec{H}\vec{S}_{\mu\nu}}{\Phi_0}+k_\xi \quad (11)$$

or

$$\Psi_{ex}\rightarrow\Psi_{ex}+\frac{k_\xi}{s_\xi}, \quad (12)$$

where the s_ξ' s are the nonnull components of the unit vector $\hat{H}$ in the external field direction. This analysis shows that, in the case only one component s_ξ is different from zero ($s_\xi=1$), we have $\Delta\Psi_{ex}=1$. On the other

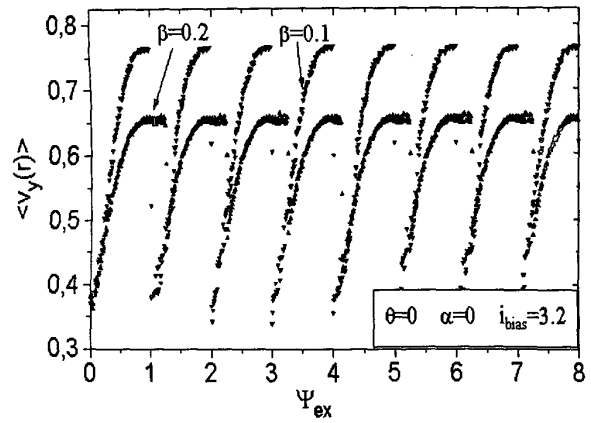

Fig. 5. Average normalized voltage $< v_y(\vec{r}) >$ versus the normalized applied flux Ψ_{ex} for α=0, $\theta = 0$, $i_{bias} = 3.2$ and for: $\beta = 0.1$; $\beta = 0.2$.

hand, if there are two nonnull components of $\hat{H}$ (let us say s_x and s_z), then $\Delta\Psi_{ex}$=k_x/s_x=k_z/s_z, thus requiring s_x/s_z to be a rational number. Following this type of reasoning, we have $\Delta\Psi_{ex} = 1$ for $\alpha = 0$ and $\theta = 0$, and $\Delta\Psi_{ex}$=$\sqrt{2}$ for $\alpha = 0$ and $\theta = \pi/4$, as it appears from Figs. 2*b*, 3*b*. It is not always possible to detect a simple periodicity $\Delta\Psi_{ex}$, as, for example, in the case of $\alpha = 0$ and $\theta = \pi/6$. In Fig. 4*a* we show the time dependence of the same three voltages of Figs. 2*a*, 3*a* for $\alpha = 0$, $\theta = \pi/6$, $\beta = 0.2$, $i_{bias} = 3.2$ and $\Psi_{ex} = 1.8$. In Fig. 4*b* we report the time average of these voltages as a function of Ψ_{ex} for the same choice of β and i_{bias} as in Fig. 4*a*. While the time dependence of the voltages $v_x(\vec{r}+a\hat{z})$, $v_y(\vec{r})$ and $v_z(\vec{r})$ show a clear periodicity in time, their time-averaged values plotted in terms of Ψ_{ex} loose the regular behavior of the curves in Figs. 2*b*, 3*b*. However, as (11), (12) imply, at least a quasiperiodic dependence on Ψ_{ex} is always present. This point clearly opens the way for further investigation on the structures appearing in the $< v_\xi >$ vs. Ψ_{ex} curves for irrational ratios of the field components.

In Fig. 5 we finally show the dependence of the average voltage $< v_y(\vec{r}) >$ on an axial magnetic field for a value of the parameter β ($\beta = 0.2$) greater than that of the corresponding curve in Fig. 2*b* and for the same choice of other parameters as in Fig. 2*b*. From these curves we may see that the system behaves like a dc SQUID, showing a decrease of the average normalized voltage for increasing β values at a fixed Ψ_{ex} and i_{bias} [8].

From the above results we argue that the cubic network of JJs shows time periodicity in the voltages across its twelve branches. Fixing the current bias, this time periodicity depends on the applied field direction. Moreover, the averaged voltages plotted as a function of the field intensity present periodicities in the case the non-zero field components are commensurate. This behavior, though being similar to that of a SQUID, depends on the field direction in a predictable way. One can thus envision future applications of these systems as vectorial sensors mainly in two ways. The first consists in extracting the external field intensity and direction from the system's electrodynamic response by solving an inverse type of problem. The second consists in allowing the network to rotate in space in a controlled way until a predefined known response is achieved. In this second case, though, one has to take care of choosing the model parameters in such a way to have a reversible magnetic response for every field direction [**10**].

IV. Conclusion

We have studied the magnetic field response of a current biased three-dimensional cubic network of inductively coupled JJs. The voltage across the branches of the network has been numerically calculated, for fixed values of the external forcing terms i_{bias} and Ψ_{ex} and for different field directions, as a function of time. The time average of the above voltages has also been reported as a function of Ψ_{ex}. These results show that the system's electrodynamic response depends in a predictable way on the external field direction, making the cubic network a valid candidate for a sensitive vectorial magnetic field sensor.

Acknowledgment

We thank Prof. S. Pace for many helpful discussions.

References

[1] S. Tanaka, H. Itozaki, and H. Toyoda, N. Harada, A. Adachi, K. Okajima, and H. Kado, T. Nagaishi, "Four-channel $YBa_2Cu_3O_{7-\delta}$ dc SQUID magnetometer for biomagnetic measurements," *Appl. Phys. Lett.* vol. **64**, pp. 514-516, 1994.

[2] H. - J. Krause, Y. Zhang, R. Hohmann, M. Gruneklee, M. I. Faley, D. Lomparski, M. Maus, H. Bousack, and A. I. Braginski, "Eddy current aircraft testing with mobile HTS-SQUID gradiometer system," *Inst. Phys. Conf. Ser.* No **158**, pp. 775-780, 1997.

[3] E. Dantsker, D. Koelle, A. H. Miklich, D. T. Nemeth, F. Ludwig, and J. Clarke, "High-T_c three-axis dc SQUID magnetometer for geophysical applications," *Rev. Sci. Instrum.* vol. **65**, pp. 3809-3813, 1994.

[4] A. P. Rijpma, Y. Seppenwoolde, H. J. M. ter Brake, M. J. Peters, and H. Rogalla, "Application of SQUID magnetometers in fetal magnetocardiography," *Inst. Phys. Conf. Ser.* No **158**, pp. 771-774, 1997.

[5] R. Weidl, S. Brabetz, F. Schmidl, F. Klemm, S. Wunderlich, and P. Seidel, "Heart monitoring with high-T_c d.c. SQUID gradiometers in an unshielded environment," *Supercond. Sci. Technol.* vol. **10**, pp. 95-99, 1997.

[6] K. K. Likharev, "Dynamics of Josephson junctions and circuits," Gordon and Breach Science Publishers, New York, 1984.

[7] C. D. Tesche and J. Clarke, "dc SQUID: noise and optimization," *J. Low Temp. Phys.* vol. **29**, pp. 301-331, 1977.

[8] A. Barone and G. Paterno', "Physics and applications of the Josephson effect," Wiley, New York, 1982.

[9] R. De Luca and T. Di Matteo, A. Tuohimaa and J. Paasi, "Three-dimensional Josephson-junction arrays: Static magnetic response," *Phys. Rev. B* vol. **57**, pp. 1173-1180, 1998.

[10] B. A. Glowacki, J. Jackiewicz and J. E. Evetts, "Angular reversibility and irreversibility of critica current in polycrystalline $YBa_2Cu_3O_7$ wires," *Cryogenics* vol. **33**, pp. 86-90, 1993.